Supporting Information for

Toward High-Performance Li-rich $Li(Ni_xCo_yMn_z)O_2$ Cathodes: Facile Fabrication of Artificial Polymeric Interphase using Functional Polyacrylates

Bing Sun,[a] Mario El Kazzi,[a] Elisabeth Müller,[b] Erik J. Berg[a]

[a]*Electrochemical Energy Storage Section, Electrochemistry Laboratory, Paul Scherrer Institute, 5232 Villigen PSI, Switzerland*

[b]*Electron Microscopy Facility, Paul Scherrer Institute, 5232 Villigen PSI, Switzerland*

Table S1. Binding energy assignments of curve fitted peaks from XPS spectra.

Components	Binding energy [eV]			
	C1s	O1s	F1s	TM/Li
LiPAA	288.7 (O-C=O) 285.2 (hydrocarbon)	533.2 (C-O) 531.8 (C=O)		55.7
HE-NCM	288.5 (O-C=O) 287.7 (C-O)	533.2 (C-O) 531.8 (C=O) 529.6 (TM-O)		54.3 (Li1s) 67.3, 73.1 (Ni3p) 61.0, 71.0 (Co3p) 49.7 (Mn3p)
PVdF	290.5 (CF_x) 286.3 (CH_2)		687.8 (CF_x) 684.7 (LiF)	
SC65	284.4 (C-C)			
Al_2O_3		532.4		

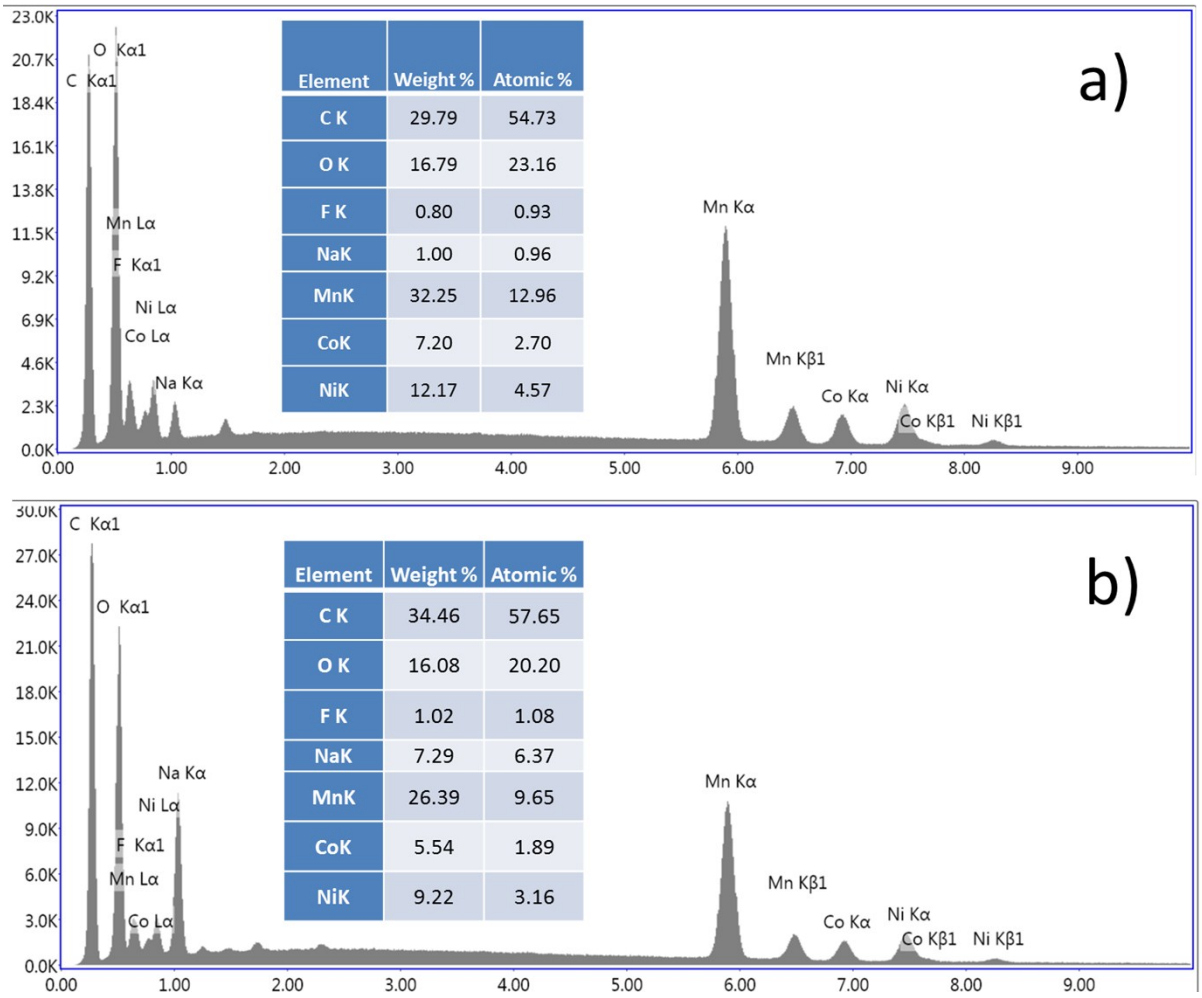

Figure S1. EDX mapping results of (a) 0.5% and (b) 5% NaPAA-coated HE-NCM cathodes.

The concentrations shown here are not giving the effective concentrations of the materials. Nevertheless, they illustrate the increasing thickness of the coating layer on top of the electrode, as can be deduced from the relative increase of the Na-signal.

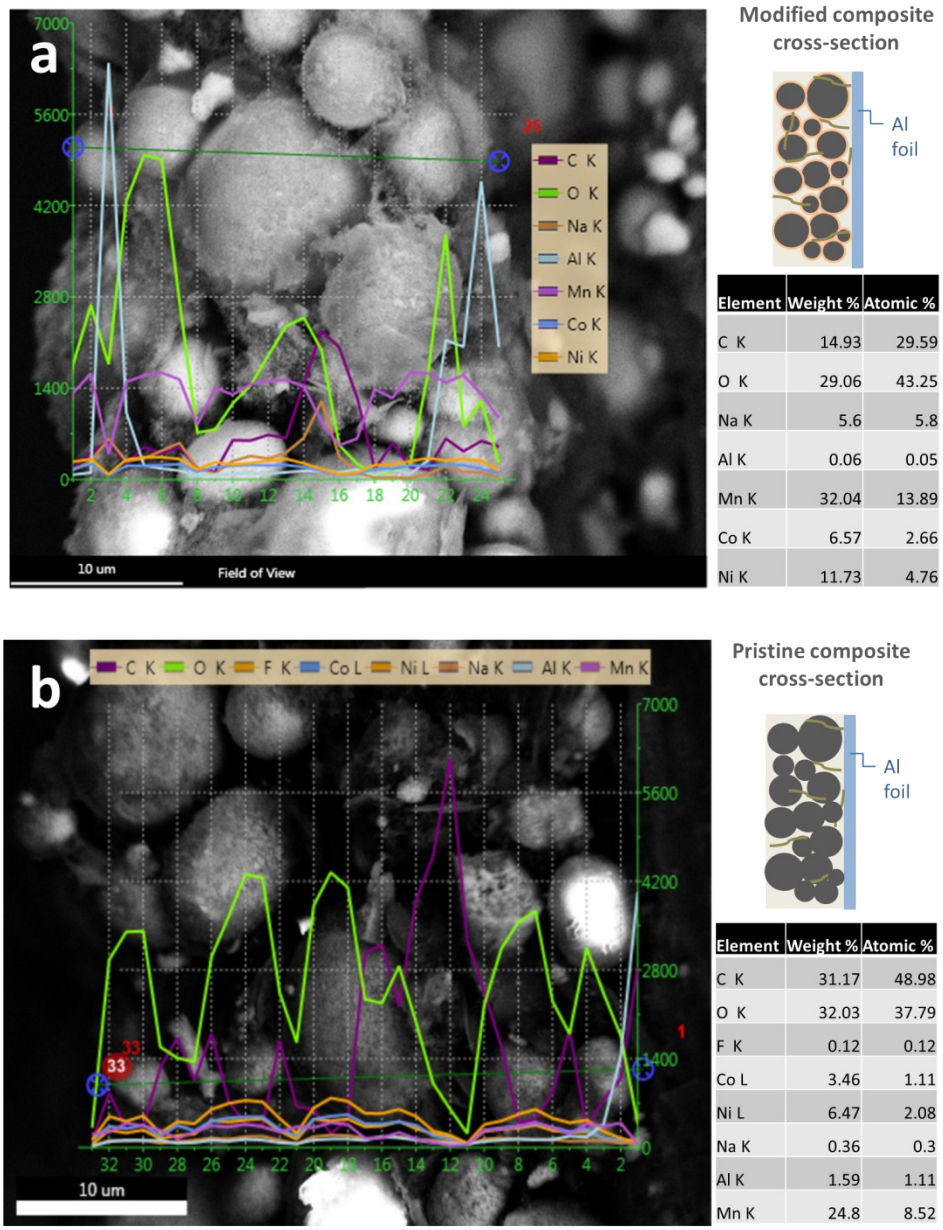

Figure S2. SEM/EDX mapping results showing the line-scanning along the cross-sections of (a) NaPAA-coated HE-NCM cathodes with 5% NaPAA loading; (b) pristine HE-NCM cathodes.

The Na-signal was traced from the cross-sections of both 5% coated (Fig. S2a) and pristine (Fig. S2b) composite electrodes by line-scanning EDX analysis. In consistent with the concentration mapping results from the top of the 5% coated composite samples (Fig. S1b), the relative increase of the Na concentration as compared to the pristine electrode suggests increasing thickness of the coating layer across the cross-section of the coated electrodes. Furthermore, by tracking the Na-signal (in dark brown line) in Fig. S2a, NaPAA coating could be detected across the cross-section which reaching to the bulk composite electrodes. It could also be seen that the relative intensity of Na- and Mn-signals appears to follow the same pattern across the electrode cross-section.

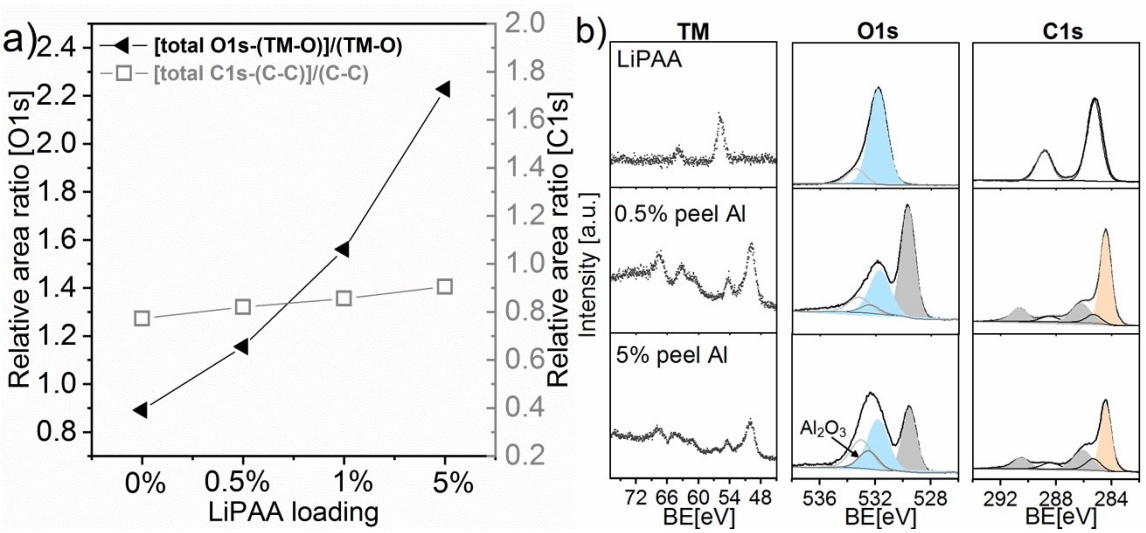

Figure S3. (a) The relative area ratios extracted from [total O1s-(TM-O)]/(TM-O) from O1s spectra (solid triangle) and [total C1s-(C-C)]/(C-C) from C1s (open square) spectra, respectively; (b) XPS spectra showing the elemental fittings of LiPAA, 0.5% and 5% LiPAA-coated HE-NCM cathodes and the same samples peeling off from the Al current collector.

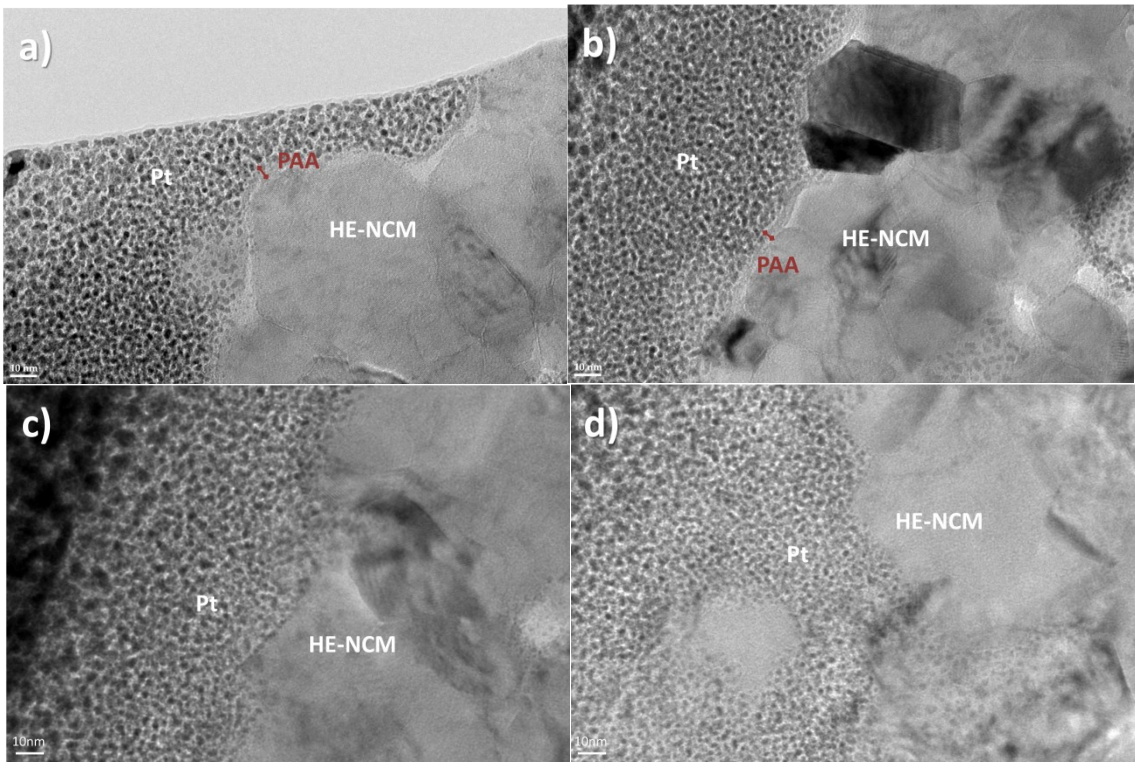

Figure S4. TEM images of (a-b) 5% LiPAA-coated and (c-d) pristine HE-NCM samples.

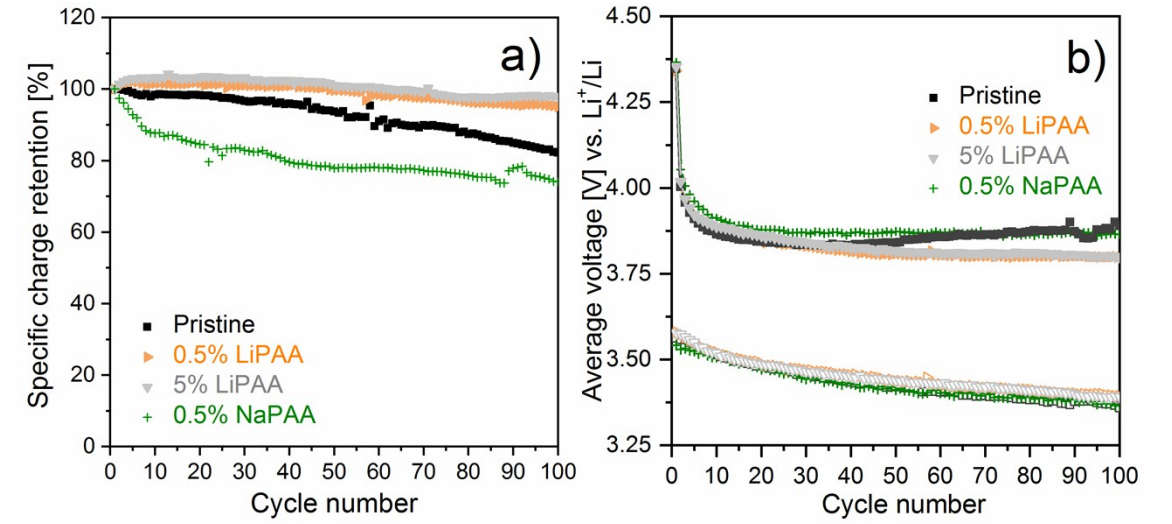

Figure S5. (a) Specific charge retention of pristine and MPAA-coated HE-NCM (M=Li, Na) cathodes vs. Li within 2.0–4.7 V; (b) the corresponding average voltages as a function of cycle number.

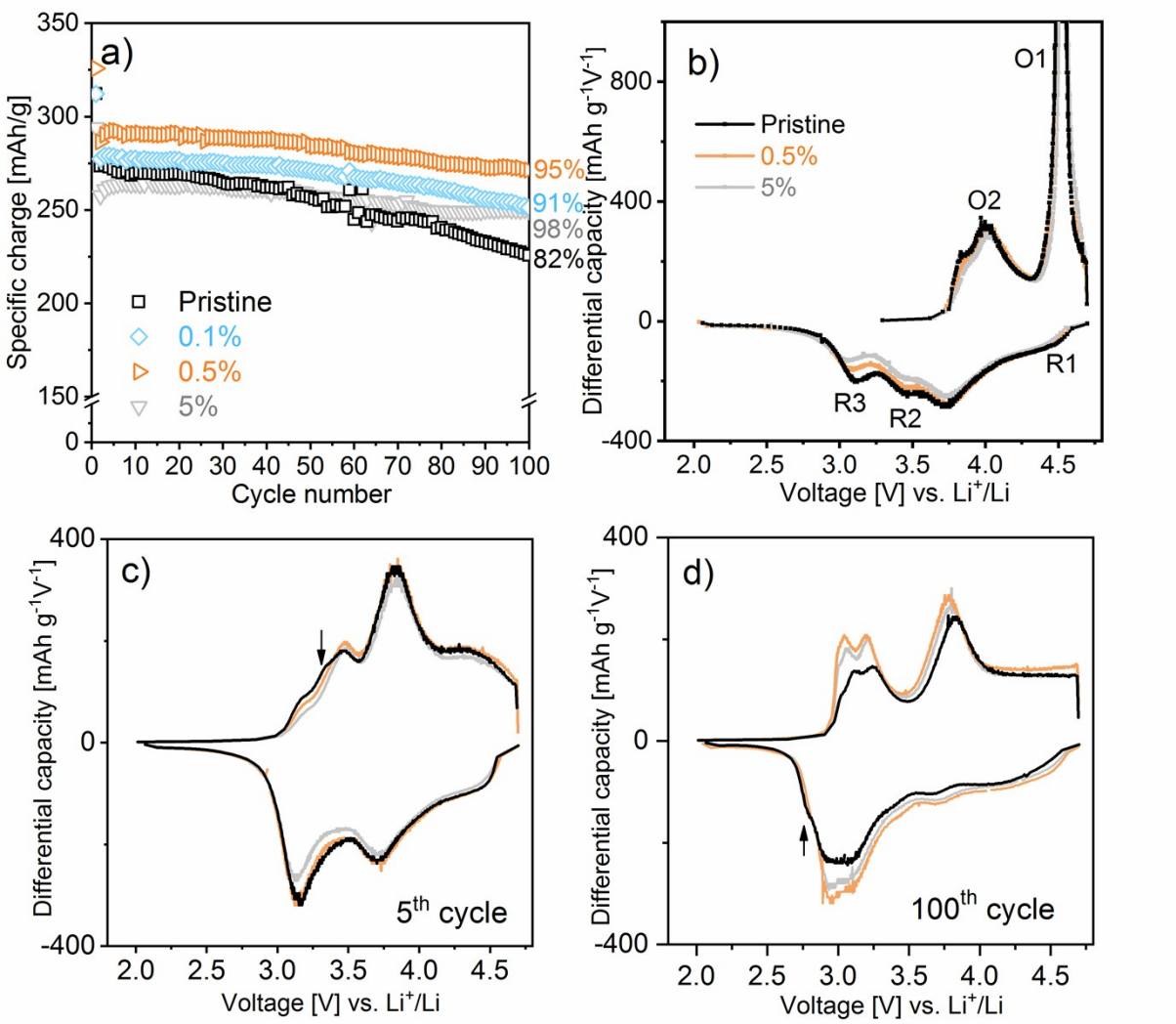

Figure S6. (a) Specific charge of the pristine and coated HE-NCM cathodes (0.1%, 0.5% and 5% LiPAA loadings) between 2.0–4.7 V vs. Li^+/Li at C/10 rate, with the corresponding capacity retention

percentages at the 100th cycle indicated; differential capacity dQ dV^{-1} plots of (b) 1st cycle (c) 5th cycle and (d) 100th cycle, respectively.

In Fig. S6b, the sharp peak during the 1st charge at close to 4.5 V vs. Li^+/Li (O1) was previously assigned to the de-lithiation of Li_2MnO_3 phase following by the oxidation of TM ions,[1–3] corresponding to the oxidation of O^{2-} to O^- during the process of Li^+ extraction from Li_2MnO_3 phase. At the second oxidation peak (O2) at around 4.0 V, a concomitant oxidation of TM ions follows the Li^+ extraction from the $LiMO_2$ component. During the discharge cycle, reversible O^{2-}/O^- could occur at around 4.4 V (R1).[3] The peak close to 3.7 V was attributed to Co/Ni reduction in $LiNi_{1/3}Co_{1/3}Mn_{1/3}O_2$ of the parent structure, which remained its position from all the tested cells. Indicative peaks of $MnO_2/LiMnO_2$ reduction were suggested at around 3.1 V (R2) and 3.4 V (R3), in correspondence to the reduction of Mn^{4+} to Mn^{3+} of layered oxide structure and layered-spinel structure, respectively.[3,4] Further examination of the dQ dV^{-1} plots during long cycling, *e.g.*, 5th and 100th cycles is shown in Fig. S6c,d. The progression of peaks at close to 3.3/3.6 V and 2.7/2.9 V is typical signatures of voltage decay; the latter particularly was assigned to the Mn^{4+}/Mn^{3+} reduction in spinel-like phase.[3,4] The absence of such progression from LiPAA-coated electrodes indicates an impeded growth of spinel-like phase and slower voltage decay in comparison with the case in pristine electrode.

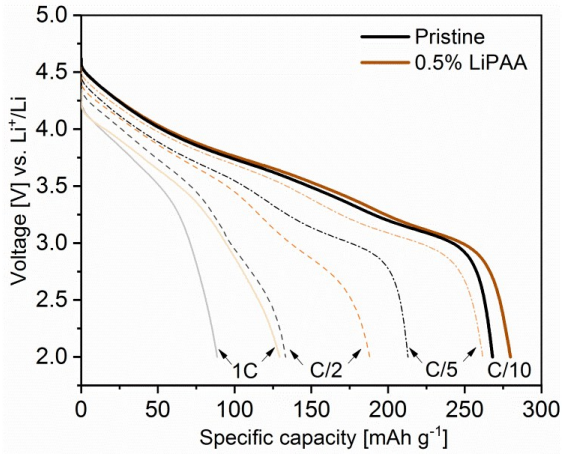

Figure S7. Galvanostatic cycling profiles from pristine and 0.5% LiPAA-coated HE-NCM cathodes at different C-rates (C/10, C/5, C/2 and 1C).

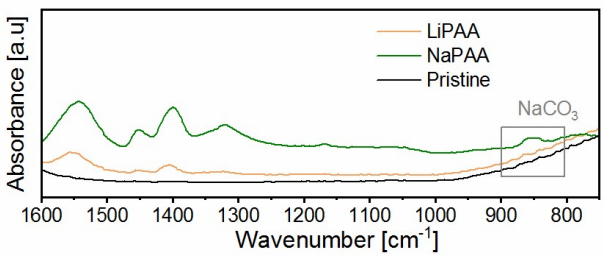

Figure S8. IR spectra of pristine, 5% LiPAA- and 5% NaPAA-coated HE-NCM cathodes.

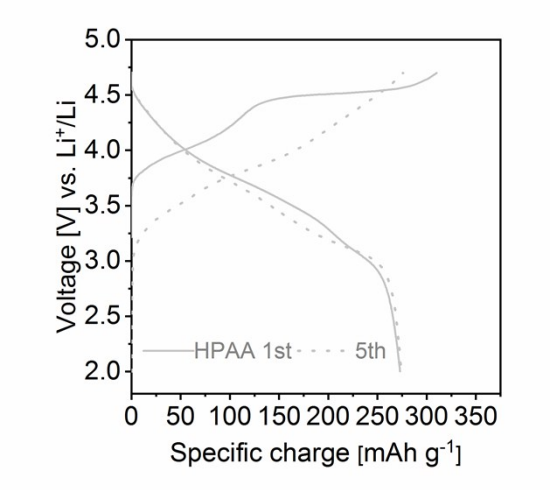

Figure S9. Galvanostatic cycling profiles of 0.5% HPAA-coated HE-NCM cathodes between 2.0–4.7 V vs. Li^+/Li at C/10 rate.

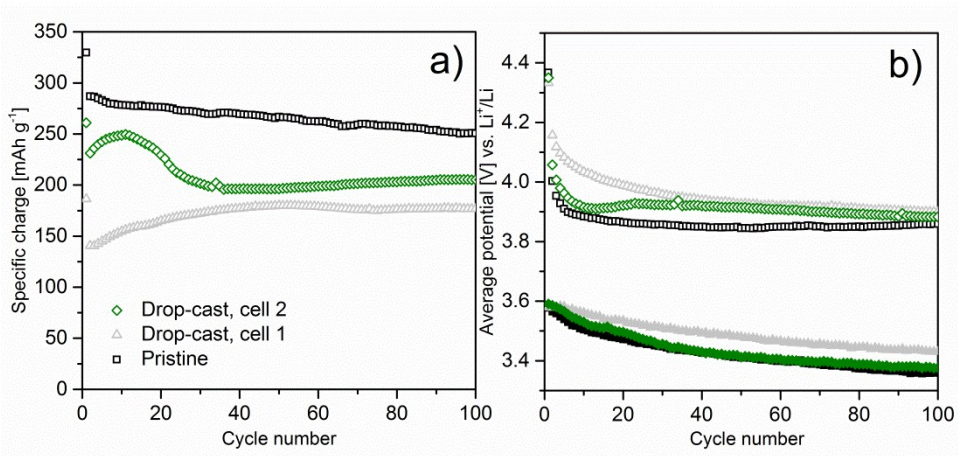

Figure S10. (a) Galvanostatic cycling profiles of pristine and 0.5% LiPAA coated HE-NCM cathodes treated by drop-casting processing; (b) the corresponding average voltage evolutions as a function of cycle number within 2.0–4.7 V at C/10 rate under 25 ±1°C.

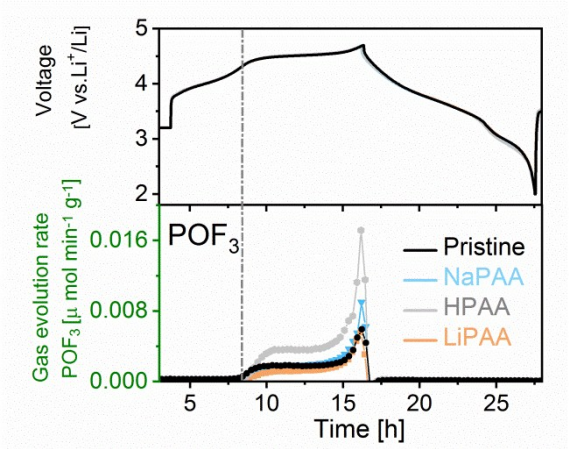

Figure S11. Gas evolution profile of POF_3 (m/z = 85) from MPAA (M = Li, Na)- and HPAA-coated electrodes at 0.5% loading in a potential range of 2.0–4.7 V vs. Li^+/Li at C/10 rate.

References

1 B. Strehle, K. Kleiner, R. Jung, F. Chesneau, M. Mendez and A. Hubert, *J. Electrochem. Soc.*, 2017, **164**, A400-406.

2 E. M. Erickson, F. Schipper, R. Tian, J.-Y. Shin, C. Erk, F. F. Chesneau, J. K. Lampert, B. Markovsky and D. Aurbach, *RSC Adv.*, 2017, **7**, 7116–7121.

3 J. Wang, X. He, E. Paillard, N. Laszczynski, J. Li and S. Passerini, *Adv. Energy Mater.*, 2016, **6**, 1600906:1-17.

4 M. Hou, S. Guo, J. Liu, J. Yang, Y. Wang, C. Wang and Y. Xia, *J. Power Sources*, 2015, **287**, 370–376.